

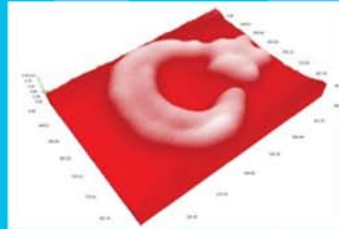


NANOMANYETİK BİLİMSEL CİHAZLAR

Türkiye'den Dünyaya Nanoteknoloji

Türkiye'nin ilk nanoteknoloji firması olarak 1999 yılında kurulan NanoManyetik Bilimsel Cihazlar, 30mK - 300K gibi geniş bir sıcaklık aralığında çalışabilen alçak ve yüksek sıcaklık Taramalı Uç Mikroskoplarının (Scanning Probe Microscope) geliştirilmesi ve üretilmesinde uzmanlaşmıştır. NanoManyetik Bilimsel Cihazlar, 50nm uzaysal çözünürlüğe kadar kalitatif ve tahribatsız manyetik görüntüleme yapabilen Taramalı Hall Aygıtı Mikroskopları'nın (Scanning Hall Probe Microscope) **dünyadaki ilk ticari üreticisidir**. NanoManyetik, son olarak geniş bir sıcaklık aralığında ve atmosferik koşullarda 10nm den daha iyi çözünürlükte manyetik görüntüleme yapabilen Manyetik Kuvvet Mikroskobu (MFM) geliştirmiştir. Yanısıra pek çok farklı yüzey özelliğinin incelenmesinde kullanılan farklı tarama kiplerini içeren, biyolojik örneklerin de incelenmesine uygun, çok amaçlı Atomik Kuvvet Mikroskopları (AKM) geliştirilmesi ve üretimi de **Türkiyede ilk defa** NanoManyetik tarafından gerçekleştirilmiştir. Ürünlerimiz, ABD, Japonya, Hindistan, Avrupa ülkeleri ve Türkiye'de pekçok saygın üniversite ve laboratuvarında kullanılmaktadır. Bunların başında **Oxford, MIT, Kyoto, Harvard** gibi tanınmış üniversiteler, **Los Alamos National Lab., TATA- Institutes** gibi araştırma kurumları ve **Seagate** gibi önemli şirketler gelmektedir. Geliştirdiğimiz AKM sistemleri ile atomic örgü ve atomik step limitlerinde görüntü alabilmekte; MFM, EFM, Conductive AFM, PFM, STM, vb. AKM çalışma modlarını sunabilmekteyiz. Sistemimize entegre ettiğimiz kapalı sıvı hücre ünitesi de biyolojik çalışmalar için eşsiz fırsatlar sunmaktadır.

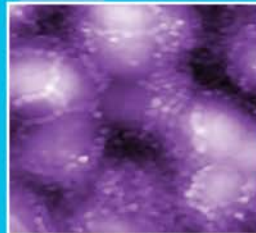
Farklı bilim dallarında eğitim görmüş yetkin personel, 4 eksenli CNC tezgah, CAD/CAM kapasitesi, test , ölçüm ve düşük sıcaklık deney düzenekleri ile tüm AR&GE faaliyetlerini, cihazların mekanik, elektronik ve yazılım kısımlarının **tamamını Türkiye'de gerçekleştiren** NanoManyetik ülkemizden tüm dünyaya teknoloji ihraç etmektedir...



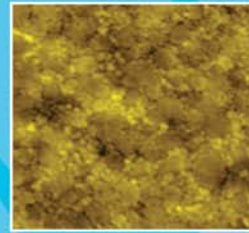
AKM Nanolitografi
Dünyanın en küçük türk bayragı
2006



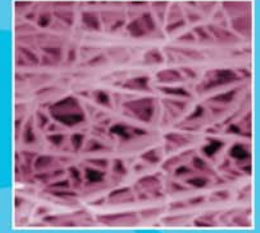
Mika atomik katmanlar



Mn katkili piezo ince film



LCMO



Polimer kaplı alüminyum



NanoManyetik Bilimsel Cihazlar Ltd
Hacettepe Teknopark ,3. ARGE , No:24
Beytepe, 06800, Ankara
Tel: 312 299 2171
bilgi@nano.com.tr www.nano.com.tr

SPECS is specialized in the development and production of **customized UHV surface analysis systems**. Following the customer's vision, SPECS conceives, designs, and produces individual systems to meet the customer's needs.

In our customized UHV surface analysis systems, sample preparation facilities like **MBE, sputtering, and thin film deposition** are combined with in-situ analysis by our ultra high resolution **XPS analyzer** PHOIBOS, by **LEED** diffraction and by imaging techniques like **STM, LT-STM, and LEEM/PEEM**. A large variety of excitation sources can be mounted on our UHV vacuum chambers. All systems are accompanied by a powerful and easy to handle software speeding up the acquisition and analysis of scientific data.

Surface science provides deep insights into the properties of matter which are indispensable when developing new products and applications for tomorrow's world: nanotechnology, information technology, medicine, materials science, environmental protection, production of energy. The research tasks require surface analysis systems of the highest standards. SPECS meets these requirements by pooling and combining the company's expertise with that of Bestec, CreaTec and Surface Concept within the Network of Competence. unavailable.



Electron Spectrometers Scanning Probe Microscopy



Sources



LEEM/PEEM



LEED



Thin Film Growth

REPRESENTED IN TURKEY BY

**NANOMANYETİK BİLİMSEL CİHAZLAR**

Hacettepe Teknokent Kuluçka Merkezi Arge Binası No : 31, 06800 Beytepe, Ankara

TEL : +90 312 299 2171

FAKS : +90 312 299 2173

www.nano.com.tr --- bilgi@nano.com.tr

Monolayer-directed Assembly and Magnetic Properties of FePt Nanoparticles on Patterned Aluminum Oxide

Oktay Yildirim,^{1,2*} Tian Gang,³ Sachin Kinge,^{3,4} David N. Reinhoudt,^{1,4} Dave H.A. Blank,² Wilfred G. van der Wiel,³ Guus Rijnders² and Jurriaan Huskens¹

¹Molecular Nanofabrication Group

²Inorganic Materials Science

³SRO NanoElectronics

⁴Supramolecular Chemistry & Technology

MESA+ Institute for Nanotechnology, University of Twente, P.O. Box 217, 7500 AE, Enschede, The Netherlands

Abstract— Modification of Al₂O₃ surfaces with self-assembled monolayers (SAMs) of phosph(on)ates with terminal functional groups resulted in FePt NPs assembly via ligand exchange. Patterning the substrates by microcontact printing allowed local nanoparticle assembly. Thermal annealing led to phase transformation of the NPs which resulted in ferromagnetic behavior at room temperature. By nanoimprint lithography FePtAu patterns at micron and nanoscale with high contrast between patterned and non-patterned regions were created. Electrical measurements showed that SAM formed an insulating barrier on conducting metal oxide.

Recently, ferromagnetic nanoparticles have attracted great interest due to their high chemical stability, hard magnetic properties and small size which makes them good candidates to be used at spintronic devices, magnetic sensing and ultrahigh density data storage applications [1]. Synthesis, characterization and assembly of monodisperse FePt nanoparticles have been extensively studied. FePt nanoparticles have high magnetocrystalline anisotropy (10⁸ erg/cm³), which indicates, a 3nm particle has much higher magnetic anisotropy energy than the thermal energy[1]. They have higher chemical stability than other hard magnetic materials[1]. Their well defined boundaries and small size are

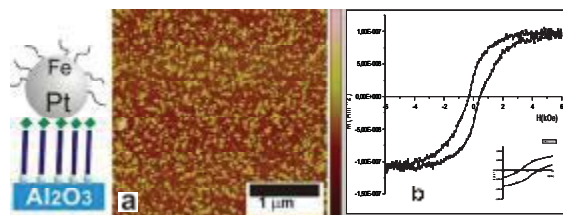


Figure 1: (a) AFM of FePt nanoparticles assembled on ABP/Al₂O₃ surface. (b) VSM of FePt nanoparticles assembled on PEI/Al₂O₃ surface and annealed at 800°C under H₂/N₂ environment.

very suitable to have storage densities in order of terabit/inch² with reduced noise.

To be able to use FePt nanoparticles having high magnetocrystalline anisotropy for magnetic data storage applications, it is necessary to have control on the assembly process and cover a sizeable area with high packing density.

Although most of the study has been done on FePt NPs on SiO₂ substrates, Al₂O₃ is a better candidate to be used as substrate instead of SiO₂ because Al₂O₃ is an important dielectric material used in electronic device fabrication and the mostly used dielectric in magnetic tunneling junctions (MTJs) and a more electrically resistant material than SiO₂. Besides, Al₂O₃ may be a model system for other FePt/metal oxide systems.

We demonstrate a method to assemble FePt nanoparticles on Al₂O₃ surface in a controlled way via assembly and ligand exchange of FePt NPs on polyethyleneimine (PEI), aminobutyl phosphonic acid (ABP) or phosphoundecanoic acid (PNDA) modified Al₂O₃ surfaces

(Figure1). Thermal annealing under N₂/H₂ reducing environment leads to a phase change of FePt from chemically disordered FCC to chemically ordered FCT phase which results in ferromagnetic behaviour at room temperature with around 440 Oe coercivity (Figure2). Microcontact printing (μCP) provides the possibility to direct the NP assembly to designated areas of the substrate. Self-assembly combined with phosph(on)ate based PNDA, ABP, MUP self assembled monolayers (SAMs) having different end-groups is shown to be an effective tool to fabricate FePtAu patterns with high contrast between patterned and non-patterned regions with a high resolution below 200 nm as well as in micron range by using nanoimprint lithography (NIL). To use the (SAMs) in spintronic devices, to be able to fabricate electrical contacts and to have information on electrical properties of SAM layers is necessary. Electrical characterization of the SAMs on conducting metal oxide Nb doped SrTiO₃ (NbSTO) by cyclic voltammetry (CV) showed the efficiency of SAM layer to isolate the substrate from environment. Pt top contacts fabricated by pulsed laser deposition (PLD) are isolated from the substrate by SAM layer. When compared to bare NbSTO substrate, organic layer on NbSTO has similar effect with an 4 nm Al₂O₃ layer on NbSTO and causes a decrease in the leakage current at same voltage range. The authors gratefully acknowledge support from the MESA+ Institute for Nanotechnology (SRO Nanofabrication) and NanoNed, the Nanotechnology network in The Netherlands. This work is part of WGvdW's research program 'Organic materials for spintronic devices', financially supported by the Netherlands Organization for Scientific Research (NWO) and the Technology Foundation STW. We acknowledge Mark Smithers for TEM and Gerard Kip for XPS measurements. We thank A. Wagenaar and J. Engbersen (RUG, Groningen) for providing TDP.

*Corresponding author: o.yildirim@tnw.utwente.nl

[1] S. H. Sun, S. Anders, T. Thomson, J. E. E. Baglin, M. F. Toney, H. F. Hamann, C. B. Murray and B. D. Terris, *Controlled Synthesis and Assembly of FePt Nanoparticles*, J. Phys. Chem.B, 2003, 107, 5419-5425.

Magnetic Properties of Exchange Coupled Py/Cr/Py trilayer films

B. Aktaş¹, R.Topkaya¹, M.Erkovan¹, M.Özdemir¹, O.Öztürk¹
¹Gebze Institute of Technology, P.K. 141, 41400 Gebze-Kocaeli, Turkey

Abstract-The ferromagnetic thin films attracts considerable attention of researchers due to their applications in the magnetoelectronics. The exchange interactions play most important role in GMR applications. Therefore the accurate magnetic characterization of the magnetic multilayered structures is one of the key issues. As the thickness of the magnetic multi-layers reduces down to nanometer scale, then the magnetic signal to noise ratio dramatically decreases. On the other ferromagnetic resonance (FMR) was proven to be one of the well established, sensitive and useful technique. In this work, we have studied the magnetic properties of ultra-thin Ni₈₀Fe₂₀/Cr/Ni₈₀Fe₁₉ trilayer system as a function of non magnetic Cr thicknesses by using FMR and dc magnetization measurement techniques. The films were growth by conventional dc and/or rf-magnetron sputtering techniques. The Cr layer thickness is increased by 0.1 nm from 0.2 nm to 4 nm. In order to obtain the most suitable FMR signal the thickness of magnetic layers are searched to observe exchange coupling between ferromagnetic layers through non-metallic Cr layer. The FMR experiments were done by using an x-band ESR spectrometer as a function of temperature. The dc magnetic field was rotated with respect to the film in order to get information about the magnetic anisotropies and the exchange coupling parameters. The dc magnetization measurements were carried out as a function of temperature by using Quantum Design PPMS system. Two symmetrical, strong and well resolved peaks were observed. These two FMR peaks become more clear as the field orientations close to film normal. The minor peak intensity strictly depends on the orientation of the external field. When the external field direction is close to the film plane, the minor peak almost vanishes. The thickness of Cr layer was found a significant effect on the separations of the two modes in the field axis. Even the relative positions of the strong and the weak modes are interchanged for particular thickness of Cr layer. We have developed a mathematical model to analyse the FMR data of a multilayered magnetic layers separated by non-magnetic spacer but still have remarkable exchange coupling between successive layers. we have found that the exchange coupling constant change sign for every 1.1 nm steps in the spacer thickness.

Magnetic Resonance Study of Diluted Magnetic Oxide Prepared By High Temperature Cobalt Implantation in TiO₂ Rutile

S. Güler^{1*}, B. Rameev^{1,2}, R.I. Khaibullin^{2,3}, V.F. Valeev² and B. Aktaş¹

¹ Gebze Institute of Technology, 41400 Gebze-Kocaeli, Turkey

² Kazan Physical-Technical Institute of RAS, 420029 Kazan, Russia

³ Department of Physics, Kazan State University, 420008 Kazan, Russia

Abstract- The magnetic properties of “hot-implanted” ($T_{irr}=900\text{K}$) Co- and Ar-implanted single crystal TiO₂ rutile have been studied by FMR and VSM techniques. Essential effect of oxygen vacancies in Co- and Ar-implanted TiO₂, and indications of intrinsic ferromagnetism in the Co:TiO₂ have been revealed.

Further development of electronics and information technology is not possible without implementation of new functionalities. For that reason, huge research efforts are now concentrated in the field of magnetoelectronics (spintronics). This is a new very fast developing field, where the two degrees of freedom, the charge and the spin of the carriers, are utilized simultaneously. The magnetoresistance sensors made of multilayers containing metal ferromagnets, showing giant magnetoresistance (GMR) or tunneling magnetoresistance (TMR), are today’s best known successful magnetoelectronics devices [1]. However, it is commonly accepted that realization of spin-polarized current injection and manipulation in semiconductors is the key element to utilize the advantages of spintronics in full measure.

In this respect, the discovery of high-Curie temperature diluted magnetic oxides (such as transition metal doped TiO₂, ZnO, SnO₂, etc.) has attracted much attention due to their potential value in spintronic devices [2,3]. A vast number of experimental works report on the room temperature ferromagnetism observed in various oxides. However, it is still an open issue to synthesize magnetic and, at the same time, semiconducting oxides, having high Curie-temperature ferromagnetism of intrinsic origin (which is not due to cluster inclusions) [4].

In this work we studied the magnetic properties of Co-implanted and Ar-implanted single crystal (001) and (100) TiO₂ samples. Single crystalline TiO₂ rutile substrates have been implanted on the ILU-3 ion accelerator (Kazan Physical-Technical Institute) with 40 keV Co⁺ and Ar⁺ ions to a fluence of 1.50×10^{17} ions/cm² at ion current density of about 8 $\mu\text{A}/\text{cm}^2$. To obtain a homogeneous distribution of doped ions in the TiO₂ matrix the substrate temperature during the implantation has been kept as high as 900^oK.

The “hot-implanted” TiO₂ samples have been investigated by ferromagnetic resonance (FMR) at 11K-300K range and vibrating sample magnetometer (VSM) techniques. FMR spectra have been recorded by using Bruker EMX Electron Spin Resonance (ESR) spectrometer at X-band (9.8 GHz) at 11K-300K temperature range and various orientations of implanted surface with respect to the applied DC magnetic field (H). VSM measurements have been performed with use of Quantum Design PPMS (9T) system.

For the Co-implanted TiO₂ sample we have observed FMR signal from room temperature up to 45 K. We observed also a clear indication of phase transition at temperatures of 25-40 K as revealed by VSM and by abrupt change in tuning conditions through this temperature range during the magnetic resonance measurements. This effect has been attributed to an increase of the sample impedance due to charge carrier localization at low temperatures. Besides, this is accomplished by disappearance of FMR signal as well. On the other hand, below 22 K we observed paramagnetic Co²⁺ centers with the typical hyperfine splitting of ESR lines due

to nuclear spin ($I=7/2$) of Co. Our analysis shows that the ESR signal is attributed to the Co²⁺ ions substituting Ti⁴⁺ in the host TiO₂ structure. It is known that formation of Co²⁺ centers in the TiO₂ rutile involves charge compensation by oxygen vacancies. Formation of oxygen vacancies is also an additional effect of the ion radiation induced damage of TiO₂ lattice. The effect of oxygen vacancies have been studied separately in the Ar-implanted TiO₂ samples. We observed a phase transition at nearly same temperature range in the Ar-implanted samples as well. An appearance of additional signals at lower temperatures is also observed and attributed to Ti³⁺ centers formed near oxygen vacancies. Our previous studies [5] reveal a transition in the electrical resistance of both Ar and Co implanted samples in the same temperature range. Thus, our studies confirm an essential role of oxygen vacancies in the ferromagnetism observed in the Co-implanted TiO₂ rutile. Our experimental studies also points to the intrinsic origin of ferro magnetism observed in the “hot-implanted” samples.

This work was partially supported by DPT (State Planning Organization of Turkey) project no 2009 K 120730, by RFBR Grant no. 07-02-00559-a, and by joint TUBITAK-RFBR Programme, Grant No. 10-02-91225-CT, and Russian Federal Agency on Education, contract P902.

*Corresponding author : sumeyra@gyte.edu.tr

[1] F. Matsukura, H. Ohno, T. Dietl, Handbook of Magnetic Materials, Volume 14, 2002, Pages 1-87

[2] S.A. Wolf, et al., Science 294,1488 (2001).

[3] T. Dietl, H. Ohno, F. Matsukura, J. Cibert, and D. Ferrand, Science 287, 1019 (2000).

[4] N. Akdoğan, B. Rameev, S. Güler, O. Öztürk, B. Aktaş, H. Zabel, R. Khaibullin, L. Tagirov, Appl. Phys. Lett. 95, 102502 (2009).

[5] R.I. Khaibullin, private communications.

Field cooling-induced magnetic anisotropy in exchange biased CoO/Fe bilayer studied by ferromagnetic resonance

Numan Akdoğan,^{1,2} Sinan Kazan,^{1,2} Bekir Aktaş,^{1,2} Mustafa Özdemir,³ Hasan İnam,⁴ Jörg Dudek,⁴ Mohamed Obaida⁴ and Kurt Westerholt⁴

¹ Department of Physics, Gebze Institute of Technology, 41400 Kocaeli, Turkey

² NASAM-Nanomagnetism and Spintronic Research Center, Gebze Institute of Technology, 41400 Kocaeli, Turkey

³ Marmara University, Faculty of Science and Letters, Department of Physics, 34722 Istanbul, Turkey

⁴ Institut für Experimentalphysik IV/Festkörperphysik, Ruhr-Universität Bochum, D-44780 Bochum, Germany

Abstract- Exchange-biased CoO/Fe bilayer grown on MgO (100) substrate by sputtering, studied by variable angle and temperature ferromagnetic resonance. The low temperature data exhibit a sudden onset of a field cooling-induced and shifted cubic anisotropy below the Néel temperature of CoO. This results in a two-fold uniaxial or four-fold cubic symmetry for in-plane magnetic anisotropy depending on a field cooling direction. The developed theoretical model perfectly simulates the experimental data and helps to explain the mechanism of exchange bias and magnetic anisotropies in coupled antiferromagnetic/ferromagnetic system.

The exchange-bias phenomena in coupled antiferromagnetic/ferromagnetic systems have received much attention due to its fascinating physical properties as well as large-scale technological applications [1]. Among antiferromagnetic materials, transition metal oxides like NiO and CoO have extensively been used in exchange-biased bilayers and multilayers. The lower Néel temperature and the strong magneto-crystalline anisotropy are the main advantages of CoO which allow us to do field cooling experiments and enhance the exchange bias. Recently, Fe/CoO and Co/CoO bilayers have been grown on different substrates. While various aspects of exchange bias have been examined in these studies, effect of field cooling on magnetic anisotropies and magnetodynamics have not been studied in detail.

In this work, we focus on the magnetic anisotropies of CoO/Fe bilayer epitaxially grown on MgO (100) substrate. The temperature-dependent magnetic anisotropies of the Fe layer and the easy axis of the system have been determined by using advantages of ferromagnetic resonance technique. In addition, a theoretical model is developed to simulate the experimental FMR data.

CoO/Fe bilayer was grown on MgO (100) substrate by using ion beam sputtering technique with a base pressure of $\sim 10^{-9}$ mbar. After etching the MgO substrate with Ar for 20 second, a 22 nm thick Fe layer was epitaxially grown on the top of the substrate with a pressure of 4.4×10^{-4} mbar. Finally, in order to prevent the Fe layer from ex-situ oxidation and to investigate the effect of exchange bias on magnetic anisotropies, a 10 nm thick CoO layer was deposited with a pressure of $\sim 10^{-3}$ mbar.

Temperature-dependent FMR measurements were carried out using a commercial Bruker EMX electron spin resonance (ESR) spectrometer operating in X-Band (9.8 GHz). Angular dependencies of FMR spectra have been recorded with the static magnetic field rotated either in the plane of the samples (in-plane geometry - $\theta_H=90^\circ$, ϕ_H -varied) or rotated from the sample plane to the normal (out-of-plane geometry - θ_H -varied, ϕ_H -fixed). The in-plane FMR spectra of CoO/Fe/MgO sample for the external field directions between ± 45 degrees are shown in Figure. The resonance lines of FMR spectra have a relatively small linewidth indicating a high crystallinity of the Fe film. We have observed two FMR modes in both in-plane and out-of-plane geometries. This behavior reflects the symmetry of total crystalline anisotropies.

Furthermore, we have carried out FMR measurements at low temperatures to investigate the effect of exchange bias

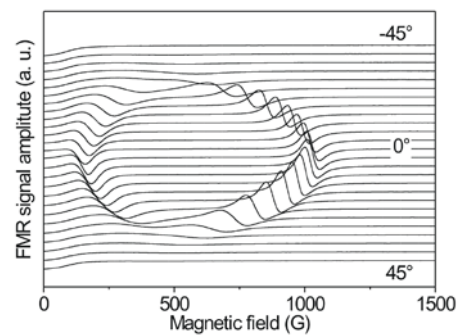


Figure 1. Some selected RT FMR spectra for the in-plane geometry.

on magnetic anisotropies. Angular dependence of resonance fields for in-plane geometry taken for field cooling under 10 kOe applied along the [010] and [011] directions. When the sample cooled along the [010] direction cubic symmetry of magnetic anisotropy still preserved. But the width of ellipses was narrowed and the resonance fields at 0 and 180 degrees were decreased compared to the room temperature data. When the sample cooled along the [011] direction, the resonance fields at 0 and 180 degrees completely disappeared. In addition, reduction of resonance fields at 90 and 270 degrees were observed. This data nicely show the strong effect of exchange bias on in-plane magnetic anisotropies of Fe film.

We would like to acknowledge P. Stauche for technical support. This work was partially supported by DPT (State Planning Organization of Turkey) through the project No 2009K120730, DFG through SFB 491 and BAPKO project of Marmara University (FEN-KPS-100105-0073). S. Kazan acknowledges TUBITAK for financial support during his postdoctoral studies at Ruhr-Universität Bochum.

*Corresponding author: akdogan@gyte.edu.tr

[1] W. H. Meiklejohn and C. P. Bean, Physical Review 102, 1413 (1956).

Dilute Magnetic Semiconductors: Combined Density Functional Theory and Quantum Monte Carlo Approach

Nejat Bulut^{1*}

¹*Department of Physics, Izmir Institute of Technology, Gulbahce, Urla 35430, Izmir, Turkey*

Abstract- In order to investigate the origin of ferromagnetism in the dilute magnetic semiconductors, we study the Haldane-Anderson model by combining the density functional theory with the quantum Monte Carlo technique.

We use the Haldane-Anderson model to discuss the substitution of transition-metal impurities into semiconductors. We study this model with the Hirsch-Fye Quantum Monte Carlo (QMC) technique in the dilute limit. The QMC results show that the occupation of the impurity bound state plays an important role in determining the nature and the range of the magnetic correlations between the impurities [1] in agreement with the Hartree-Fock predictions [2]. In order to make direct comparisons with the experimental data, we combine the Density Functional Theory (DFT) with the QMC technique. In particular, we first use the density-functional theory to calculate the host band structure and the impurity-host hybridization matrix elements, which are input parameters for the Haldane-Anderson model, and then perform the QMC simulations with these realistic model parameters [3]. For the case of (Ga,Mn) As, the DFT+QMC approach leads to an impurity bound state located ~ 100 meV above the top of the valence band in agreement with the experimental value of 110meV. In addition, we observe an anisotropic distribution of the local density of states at the impurity-bound state energy, which is consistent with the STM data. Hence, we think that the DFT+QMC approach is a useful tool for performing realistic calculations for the various compounds of dilute magnetic semiconductors.

*Corresponding author: nejatbulut@iyte.edu.tr

[1] N. Bulut, K. Tanikawa, S. Takahashi, and S. Maekawa. Long-range ferro magnetic correlations between Anderson impurities in a semiconductor host: Quantum Monte Carlo simulations, *Physical Review B* **76**, 045220 (2007).

[2] M. Ichimura, K. Tanikawa, S. Takahashi, G. Baskaran, and S. Maekawa, *Foundations of Quantum Mechanics in the Light of New Technology (ISOM-Tokyo 2005)*, eds. S. Ishioka and K. Fujikawa, World Scientific, Singapore, pp. 183–186, 2006.

[3] Jun-ichiro Ohe, Yoshihiro Tomoda, Nejat Bulut, Ryotaro Arita, Kazuma Nakamura, and Sadamichi Maekawa. Combined approach of density functional theory and quantum Monte Carlo method to electron correlation in dilute magnetic semiconductors, *Journal of the Physical Society of Japan* **78**, 083703 (2009).

Quantum-chemical study of structure and properties of gold clusters: bridging the gap between model and real gold catalysis

Pichugina D.A.^{1,2}, Beletskaya A.V.¹, Mukhamedzyanova D.F.¹, Askerka M.S.¹, Shestakov A.F.², Kuz'menko N.E.¹

¹ Department of Chemistry, M.V. Lomonosov Moscow State University, Moscow, Russia

² Institute of Problems of Chemical Physics RAS, Chernogolovka, Russia

Abstract—The nature of active sites and activity of gold containing catalysts have been studied in direct hydrogen peroxide formation and allylic allylbenzene isomerization using modern quantum-chemical methods. Au₄, Au₈, Au₁₀, Au₂₀ clusters have been chosen as a model of active gold nanoparticle. Theoretical evidence reveals that the efficiency of catalyst depends on charge and structure of gold clusters, the corner and edge gold atoms on surface play the principal role.

Nowadays, gold nanoparticles have attracted intent attention of researchers owing to prospects of use in electronic devices, medicine, functional nanoscale materials, but one of the most promising field is catalysis [1]. The application of gold catalysts makes it possible to substitute currently used polluted processes in industry for environmentally appropriate technologies. In spite of gold nanoparticles have been studied more than twenty years the nature of active sites of these catalysts and the way of oxygen and hydrogen activation on gold clusters have not been studied enough. The development and application of modern quantum-chemical methods for structures description and simulation of catalytic properties of small gold particles is a crucial task.

To clarify the mechanism of gold containing catalytic reactions the simulation of oxidation and hydrogenation process, hydrocarbons isomerization have been carried out. Structures of Au₄, Au₈, Au₁₀, Au₂₀ clusters have been chosen as a model of active gold nanoparticle. Quantum-chemical methods (MP2, CCSD, DFT/PBE, non-relativistic with pseudopotential sbk and scalar-relativistic approaches [2]) have been used.

The activation of oxygen and hydrogen on a model cluster Au₈ and mechanism of hydrogen atoms migration on gold

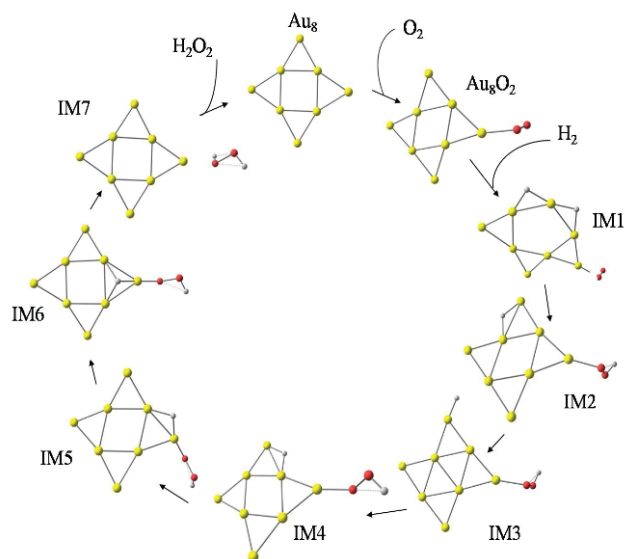


Figure 1. Catalytic cycle of direct hydrogen peroxide formation

cluster to form H₂O₂ have been investigated. The oxygen adsorption on Au₈ cluster with Au₈-O-O complex formation is the first step in catalytic cycle (Figure 1). In case of hydrogen dissociative adsorption takes place to form IM1 intermediate. The H-migration passes through 5 steps over IM2 – IM7 intermediates. The final step in this catalytic cycle is the

desorption of hydrogen peroxide molecule. It has been shown that the H-migration on gold cluster deals with low energy barriers (not higher than 85 kJ/mol). Obtained data have been compared with the alternative mechanisms of H₂O₂ synthesis on model Au₃ and Au_n⁻¹ and Au_n⁺¹ clusters [3].

For better understanding the nature of active sites we have simulated allylic isomerization of allylbenzene to cis- and trans- 1-phenylpropene catalyzed by gold nanoparticles. The model systems including allylbenzene and Au_n^z (where n=1, 4, 20, 21; z= -1, 0, +1) have been examined. The mechanism of this reaction involves the formation of a gold hydride complex. The limited rate constant of the investigated reaction depends on gold charge and increases in the following range: Au⁰ < Au⁻¹ < Au⁺¹, equal 5,5·10⁻¹³ s⁻¹, 2,8·10⁻⁷ s⁻¹ and 8,5·10⁻⁵ s⁻¹ correspondingly. Thus charged atoms are the most active on catalyst's surface. The optimized structures of reagents and products with cluster Au₂₁⁺ have shown the principal role of the corner and edge atoms in catalysis. The difference of calculated kinetic characteristics in the formation of cis- and trans- 1-phenylpropene as well as the possibility of hydride

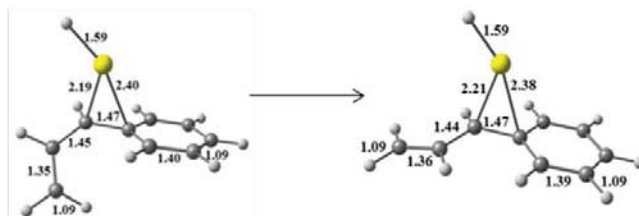


Figure 2. The isomerization of hydride complex

complex to isomerize (Figure 2) is the evidence of significant formation of trans- product [4].

Application of quantum-chemical methods to predict gold clusters properties allows us to elucidate direct hydrogen peroxide formation and allylic isomerization mechanisms. The calculations reveal that the atoms in cluster's apex have the highest activity; they are like active sites of catalyst. The obtained information can provide the impetus for further experimental studies of gold nanoparticles structure and their catalytic activity.

*Corresponding author: ITdaria@phys.chem.msu.ru

[1] A.S.K. Hashmi and G.J. Hutchings, *Angew. Chem., Int. Ed.*, 45, 7896 (2006)

[2] K.G. Dyal, *J. Chem. Phys.*, 100, 2118 (1994).

[3] A.M. Joshi, W.N. Delgass and K.T. Thomson, *J. Phys. Chem. B*, 109, 22392 (2005).

[4] V.V. Smirnov, S.A. Nikolaev et. al., *Kinet. Catal.*, 48, 265 (2007).

Transport Properties of Magnetic Tunnel Junctions with Half-metallic Ferromagnetic Electrodes

Syed Rizwan¹, S. Zhang², Z. C. Wen¹, Y. G. Zhao², and X. F. Han^{1*}

¹State Key Laboratory of Magnetism, Institute of Physics, Chinese Academy of Sciences, Beijing 100190, China

²Department of Physics, Tsinghua University, Beijing 100084, China

Abstract—We have investigated the transport properties of magnetic tunnel junction (MTJ) with the structure: STO (sub.)//LSMO (50)/MgO (1.2)/LSMO (30), all thicknesses are measured in nm. The Curie temperature (T_c) of the bottom LSMO film was around 350 K and that of the top LSMO electrode was around 270 K. The tunneling magnetoresistance (TMR) ratio of this structure is the highest value ever reported with LSMO as magnetic electrodes in MTJs at room temperature. Surprisingly, the TMR increases with increase in temperature until it reaches the T_c of the bottom LSMO electrode after that, the TMR decreases. The maximum TMR ratio of 43% is obtained at $T = 350$ K. The high TMR ratio above the T_c of the top electrode suggests that the two electrodes are strongly coupled with each other and the TMR strongly depends on the contribution from the bottom LSMO electrode at higher temperatures.

Magnetic tunnel junctions (MTJs) have attracted much attention in recent years owing to their high tunneling magnetoresistance ($TMR = (R_{ap} - R_p)/R_p$, where, R_{ap} and R_p are the junction resistances when the magnetizations of the two FM electrodes are anti-parallel and parallel with respect to each other, respectively) ratios and capability for applications in next generation data storage devices [1]. It consists of an insulating barrier, sandwiched between two ferromagnetic (FM) layers. The TMR ratio of an MTJ depends not only on the insulating barrier but also on the FM-insulator interface [2]. In 2001, W. H. Butler et al. predicted a TMR ratio of as high as 10,000% at room temperature in MTJs with crystalline MgO as the tunnel barrier [3]. On the other hand, $La_{0.67}Sr_{0.33}MnO_3$ (LSMO) was experimentally observed to be a half-metal and ferromagnet with high spin-polarization at the Fermi level [4]. Unfortunately, the TMR obtained in MTJs exploiting LSMO as the FM electrodes remained very low at high temperatures owing to their low Curie temperature T_c [5]. Thus, the low T_c of LSMO limits its practical use in the spintronic devices.

In this work, we address this issue by fabricating an MTJ with a relatively new structure: STO (sub.)//LSMO (50)/MgO (1.2)/LSMO (30)/IrMn (15)/Ta (15)/Ru (10), all thicknesses are represented in nm. We found that the TMR values do exist at low temperatures and surprisingly, it increases with increasing temperature. The highest TMR obtained at high temperature of 350 K is over 43%. The transport properties were measured by using four-probe inelastic electron tunneling spectroscopy (IETS) and the magnetic properties were observed using physical property measurement system (PPMS) and superconducting quantum interference device (SQUID).

The single LSMO (50 nm) film, used here as the bottom electrode, showed good surface morphology as confirmed by the atomic force microscope (AFM). This film has a high T_c value of 350 K. Also the MgO insulating layer that we have used in our structure has good single-crystalline structure. Figure shows the typical nonlinear current-voltage characteristics of the tunnel junction at a lower temperature of 30 K. It is clear that the I-V curve is changed when a magnetic field of 7T was applied. The different I-V curves for parallel and anti-parallel alignment of the FM electrodes clearly indicates that the junction resistance was changed when a magnetic field is applied. Thus, gives the signature of TMR present at 30 K.

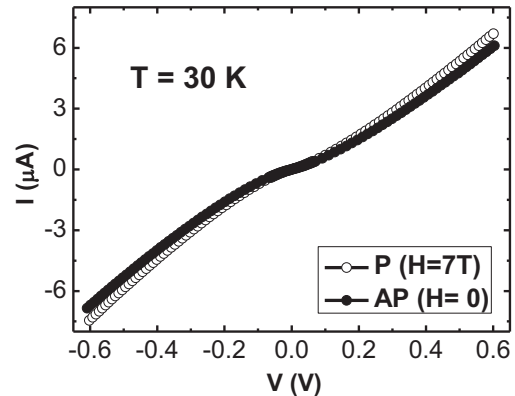


Figure: Current vs. voltage curves of LSMO/MgO/LSMO based magnetic tunnel junction in the absence (shown with solid circles), and in the presence of magnetic field of 7 tesla (shown with open circles), respectively.

When the measuring temperature was increased, the TMR was found to increase as well and reaches a highest value of 43% at a higher temperature of 350 K. This is surprising as in the normal case, the TMR is assumed to decrease with rise in temperature. In order to explore this unusual TMR behavior, we further investigated the temperature dependence of the bottom electrode resistance. We found that the maximum TMR is present at the same temperature as that of the Curie temperature of the bottom electrode. Also, the resistance vs. temperature curve for the bottom electrode showed that the increase in TMR with increase in temperature is actually originating due to contribution from the bottom electrode. This explains the reason of decrease in TMR at above 350 K, which is the Curie temperature of bottom LSMO electrode.

In summary, we presented a new structure for MTJ fabrication using LSMO as the FM electrodes and MgO as the tunnel barrier. This structure improved the Crystallinity of LSMO so that its Curie temperature remained the same as that of the bottom film, when used in the MTJ.

*Corresponding author: riz.uet@gmail.com

- [1] Lixian Jiang, Hiroshi Naganuma, Mikihiro Oogane, Yasuo Ando, Appl. Phys. Exp., **2**, 083002 (2009).
- [2] Jose Maria De Teresa, Agnès Barthélémy, Albert Fert, Jean Pierre Cpmtour, François Montaigne, Pierre Seneor, Science **286**, 507 (1999).
- [3] W. H. Butler, X.-G. Zhang, T. C. Schulthess, Phys. Rev. B, **63**, 054416 (2001)
- [4] M. Bowen, M. Bibes, A. Barthélémy, J.-P. Contour, A. Anane, Y. Lemaître, A. Fert, Appl. Phys. Lett., **82**, 233 (2003).
- [5] Syed Rizwan, S. M. Guo, Y. Wang, Z. C. Wen, S. Zhang, Y. G. Zhao, J. Zou, X. F. Han, IEEE Transaction on Magnetics (in Press).

Current enhancement and negative differential conductance in parallel quantum dots

V. Moldoveanu

National Institute of Materials Physics, P.O. Box MG-7, 077125, Bucharest-Magurele, Romania

B. Tanatar

Department of Physics, Bilkent University, Bilkent, 06800, Ankara, Turkey

Abstract We present calculations on the transport properties of few-level parallel quantum dots. Each dot is connected to non-interacting leads and the effects of the intradot and interdot Coulomb interaction are included within the random-phase approximation (RPA) implemented in the Keldysh formalism. One of the dots is weakly coupled to the leads and subjected to a small bias that allows transport through resonant tunneling. We show that by increasing the bias V on the nearby dot the inelastic Coulomb scattering modifies the current I in the first dot. More precisely, I increases when one more level of the second dot enters the bias window as electrons from the lowest levels gain enough energy to tunnel through the leads. We also show that intradot transitions in QD₁ lead to negative differential conductance (i.e., $dI/dV < 0$). The role of the lead-dot coupling and temperature is discussed. The enhancement of the current due to the energy quanta transferred from the strongly biased dot suggests a quantum ratchet or Coulomb drag mechanism.

Parallel or serially coupled quantum dot systems are ideal candidates for studying Coulomb effects on nanoscale transport. McClure et al. [1] measured the cross-current correlations for a parallel quantum dot in a four lead geometry. The experiment exploits the charge sensing effect, which relies on the mutual interaction between two capacitively coupled subsystems implying that the transport through one subsystem is affected by what happens in the nearby subsystem.

It is important to note that both dots are set in the Coulomb blockade regime and that electron tunneling between the two dots is not allowed. Therefore, the only coupling comes from the interdot Coulomb interactions. Khrapai et al. [2,3] on the other hand, reported a ratchet effect and electronic counterflow. The system considered in these experiments is a double quantum dot coupled to two leads and placed in the vicinity of a quantum point contact (QPC) which is also subjected to a finite bias. At weak interdot tunneling the levels of each dot can be detuned by an asymmetry energy such that the system is in the Coulomb blockade. The transport measurements show that electrons can pass through the double dot if the bias applied on the QPC insures an energy transfer between the two subsystem, via inelastic scattering.

Motivated by these experiments we investigate the electronic transport in parallel quantum dots. Theoretically, the description of the above-mentioned features is challenging as the mean-field approximations for the Coulomb effects are not capable of capturing the inelastic scattering processes. In this work we used the Keldysh formalism and the RPA for the Coulomb interaction effects [4] where the inelastic scattering processes are naturally included in the transport calculation.

The specific system we consider consists of two parallel quantum dots. One of the dots is set in the Coulomb blockade regime while the other one rather strongly coupled to the leads and subjected to a finite bias. We compute the steady state currents in each dot as a function of the bias applied on the active dot. The main result we report here supports the existence of a mesoscopic Coulomb drag. We were able to show that a

net current is generated in the unbiased (passive) dot when the bias on the active dot increases. This process is entirely due to the interdot interaction and to the momentum transfer between the two subsystems. As long as there is no bias applied to the active dot the imaginary part of the interaction self-energy is zero and no drag appears. The situation changes when a level of the active dot approaches and enters the finite bias window. The electrons tunnel through the dot and drag the current in the passive dot. Enlarging the bias window one collects more conduction channels through the active dot, and as a consequence the Coulomb drag is enhanced. The sawtooth behavior of the drag current shows that at some values of the bias a negative differential conductance regime is reached. We analyze the density of states of the passive dot and infer that this is due to the intradot transitions that compete with the tunneling processes.

In summary, we have employed the Keldysh-RPA scheme and studied the mesoscopic Coulomb drag in parallel quantum dots. Our results are relevant for the recent experiments [2,3] and complement calculations by Kamenev and Levchenko. [5]

Aknowledgments. This work is supported by TUBITAK (108T743) and TUBA. V.M. acknowledges the financial support from PNCDI2 program under grant No. 515/2009 and TUBITAK-BIDEP.

- [1] D.T. McClure et al., Phys. Rev. Lett. 98, 056801 (2007).
- [2] V. S. Khrapai et al., Phys. Rev. Lett. 97, 176803 (2006).
- [3] V. S. Khrapai et al. Phys. Rev. Lett. 99, 096803 (2007).
- [4] V. Moldoveanu and B. Tanatar, Phys. Rev. B 77, 195302 (2008).
- [5] A. Levchenko, A. Kamenev, Phys. Rev. Lett. 100, 026805 (2008).



HYSITRON



Nanoindentation A Practical Approach

Nanoindentation
Nanotribology

nano
Electrical
Contact
Resistance

Scanning
Nanoindentation

Acoustic
Emission
Monitoring

nanoDMA®

Direct Observation
TEM/SEM Mechanics



Analitika

Laboratuvar ve Proses
Kontrol Cih. San. Tic. Ltd. Şti.

Ataşehir Bulvarı, 42 Ada, Gardenya 7/1
Giris Kat, D:5, 34758 Ataşehir/Istanbul

T (0 216) 456 36 95 (pbx) F (0 216) 456 07 98

E info@analitika.com.tr W www.analitika.com.tr



HAAKE POLYLAB OS MODÜLER KARIŞTIRMA VE EKSTRUDER SİSTEMİ

- CANopen Bus yardımıyla bilgisayardan USB ile network bağlantısı
- Yeni sensör ve ünitelerin ilavesine açık sistem
- Otomatik yazılım ile kolay kullanım
- Yüksek performanslı sürücü ünitesi



ANAMED
ANALİTİK MEDİKAL
SİSTEMLER A.Ş.

Acarlar İş Merkezi F-Blok Kat 1 Kavacak Beykoz 34805 İSTANBUL
Tel: (0216) 331 17 06 pbx Fax: (0212) 331 17 37
E-mail: sales@anamed.com.tr

Endohedral Monometallofullerene Gd@C₈₂

Ali Sebetci^{1*} and Manuel Richter²

¹Computer Engineering Department, Zirve University, Gaziantep 27260, Turkey

²IFW Dresden, P.O. Box 270116, D-01171 Dresden, Germany

Abstract— The structure and magnetic ground state of the endohedral metallofullerene Gd@C₈₂ is confirmed by relativistic density functional calculations. The experimentally observed reduction of the magnetic moment of Gd@C₈₂ with respect to that of a free Gd³⁺ ion is explained by a small hybridization between unoccupied Gd-4f states and carbon- π states, resulting in a presumably generic antiferromagnetic coupling of the Gd-4f spin with the remaining unpaired spin in the hybridized molecular orbital.

Rare-earth (RE) based metallofullerenes like RE@C₆₀, RE@C₈₂, and RE₃N@C₈₀ have recently attracted a wide interest in chemistry, physics, and biology. Metallofullerenes are promising, e.g., for photoelectrochemical cell and for molecular memory applications as well as for the use in spintronics devices. Another important field of application might emerge in the use of magnetic, in particular Gd containing, metallofullerenes as contrast agents in magnetic resonance imaging. Therefore, endohedral monometallofullerenes of type RE@C₈₂, beside others, have been intensively studied during the last decade. Despite the considerable number of investigations published, the interaction between the metal atom and the carbon cage deserves further clarification. In particular, the electronic origin of the observed magnetic ground state of Gd@C₈₂ is not understood so far.

The aim of this work [1] is to investigate the origin of the observed $M = 7$ ground state of Gd@C₈₂ theoretically. Starting from local spin density (LSDA) and generalized gradient approximations (GGA), we include a so-called on-site correlation correction, spin-orbit coupling, and non-collinearity effects in the DFT calculations. These effects were not considered in any of the previous DFT approaches to Gd@C₈₂.

Our calculations support the findings of the most recent theoretical and experimental investigations. We optimized the geometry of Gd@C₈₂ by NWChem and obtained, as expected, a structure with C_{2v} symmetry (see Fig.) where the Gd atom is situated above the center of a hexagonal carbon ring. The calculated Gd-C bond length is 2.49 Å, while C-C bond lengths amount to 1.46 and 1.49 Å. When the calculations are repeated with a more complete basis set (6-31G*), we found a reduction of the Gd-C bond length by about 0.8% (2.47 Å) which is in agreement with Ref. [2] and a somewhat smaller reduction of the C-C bond lengths (1.46 and 1.48 Å). Since the change in the geometry of the endohedral metallofullerene with the more complete basis set is so small, we perform the additional energy calculations for different density functionals on the originally optimized structure. OpenMX optimization by GGA+U yields a very similar structure where the Gd atom locates at a position slightly off the center of the ring. These OpenMX calculations also reveal that the previously suggested two anomalous geometries have 1.7 eV higher energies than the ground state structure.

The electron energy levels of Gd@C₈₂ close to the chemical potential, obtained by the FPLO code in scalar-relativistic mode and using LSDA+U, $U = 8$ eV, are calculated for $M = 7$ and for $M = 9$. There is one almost spin-degenerate level at the chemical potential, well separated from the next lower occupied and next higher unoccupied levels by about 0.6-0.7 eV. In the $M = 7$ ground state, the HOMO is in the spin-down channel and the

LUMO in the spin-up channel. The opposite situation is found in the $M = 9$ state.

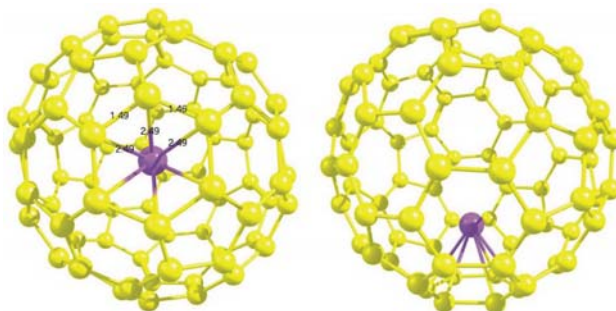


Figure: Top and side views of Gd@C₈₂ (relaxed structure). Distances are given in Angstroms.

The experimentally observed reduction of the Gd@C₈₂ magnetic moment with respect to that of a free Gd³⁺ ion is due to antiferromagnetic coupling between the 4f electrons of the Gd atom and the remaining unpaired electron on the hybridized molecular orbital. The reason for this antiferromagnetic coupling is a small hybridization of the unoccupied 4f-spin-down states with the highest occupied carbon π -states. It yields an $M = 7$ ground state that we expect to be generic for all Gd-carbon systems with unpaired electrons. For example, an $M = 7$ ground state has also been found for Gd@C₆₀ in a recent calculation [3]. Our results point to an energy difference between the $M = 7$ ground state and the $M = 9$ excited state in the order of 10 meV. While this value is larger than the value 2 meV suggested by spectroscopic data [4], susceptibility data [5] suggest an even larger value of more than 25 meV. High-temperature susceptibility measurements would be in place to clarify this open point.

We like to thank Alexey Popov, Michael Kuz'min, Klaus Koepnik, Helmut Eschrig, Gotthard Seifert, and Lothar Dunsch for discussions. Financial support has been provided by the German Science Foundation via SPP 1145.

*Corresponding author: alisebetci@zirve.edu.tr

- [1] A. Sebetci and M. Richter, *J. Phys. Chem. C*, **114**, 15 (2010).
- [2] N. Mizorogi and S. Nagase, *Chem. Phys. Lett.* **431**, 110 (2006).
- [3] R.F. Sabirianov, *et al.* *J. Phys.: Condens. Matter* **19**, 082201 (2007).
- [4] K. Furukawa, *et al.* *J. Phys. Chem. A* **107**, 10933 (2003).
- [5] H. Huang, S. Yang, X. Zhang, *J. Phys. Chem. B* **104**, 1473 (2000).